RSC Advances

PAPER

View Article Online
View Journal | View Issue

Cite this: *RSC Adv.*, 2015, **5**, 89919

Facile and expedient access to bis-coumarin–iminothiazole hybrids by molecular hybridization approach: synthesis, molecular modelling and assessment of alkaline phosphatase inhibition, anticancer and antileishmanial potential†

Aliya Ibrar,[a] Sumera Zaib,[b] Imtiaz Khan,[a] Farukh Jabeen,[cd] Jamshed Iqbal*[b] and Aamer Saeed*[a]

Received 27th July 2015
Accepted 14th October 2015

DOI: 10.1039/c5ra14900b

www.rsc.org/advances

In the design of new drugs, the hybridization approach might allow obtaining molecules with improved biological activity with respect to the corresponding lead compounds. Thus, adopting this approach, a new series of novel bis-coumarin–iminothiazole hybrids was designed, synthesized and tested for their biological action against alkaline phosphatase, leishmaniasis and cancerous cells. The structures of the synthesized hybrid compounds (**5a–m**) were characterized and established by using spectro-analytical data. The synthesized analogues were evaluated against alkaline phosphatase where compound **5j** was emerged as a potent inhibitor with IC_{50} value of 1.38 ± 0.42 μM. This inhibitory efficacy is two-fold higher as compared to the standard inhibitor. The synthesized compounds were also assayed for their anti-leishmanial potential against *Leishmania major* and compound **5i** was observed as the lead candidate with 70.4% inhibition. The prepared compounds also showed cytotoxic behavior against kidney fibroblast (BHK-21) and lung carcinoma (H-157) cancer cell lines. Molecular docking of the synthesized library of iminothiazole derivatives against ALP was performed to delineate ligand–protein interactions at molecular level which suggested that the major interacting residues in the binding sites of the proteins might have an instrumental role in the inhibition of enzyme's function. Our results inferred that compounds **5j–m** may serve as potential surrogates for the development of potent inhibitors of ALP.

Introduction

Alkaline phosphatase (ALP, E.C. 3.1.3.1.) is a non-specific phosphomonoester hydrolase that catalyzes the hydrolysis and transphosphorylation of a wide variety of organic monophosphates and regulates the functions of many biological systems.[1–3] The most common occurrence of ALP in nature suggests its involvement in fundamental biochemical processes, however, there is no positive evidence regarding its physiological functions. The possible roles of ALP have been suggested as hydrolysis of phosphoesters, phosphate transferase activity, protein phosphatase activity, phosphate transport, modulation of organic cation transport, and involvement in cell proliferation.[4,5] The biological action of the alkaline phosphatase in serum is associated with metabolic bone (hypophosphatasia) and liver diseases and also is used as a marker of osteoblastic differentiation.[6] Alkaline phosphatases may potentially be employed as therapeutic agents and show several uses in clinical medicine and in biotechnology. The most common human cancers like breast, kidney, lung and prostate have a great potential to metastasize to bone, directing towards painful and fatal consequences.[7] Bisphosphonates are widely used to reduce symptoms of osteolytic bone metastasis commonly seen in breast, kidney and lung cancer.[8] High serum level of tissue non-specific alkaline phosphatases represents elevated osteoblast activity in patients with metastatic prostate cancer.[9,10] The chemical agent that inhibit alkaline phosphatase enzyme may be useful to prevent increased osteoblast activity, commonly seen in bone metastasis.

Cancer is a notably complex, widespread and lethal disease and at present one of the most leading causes of death accounting for 7.6 million (around 13% of all deaths) in 2008, that are projected to continue rising, with an estimated 13.1 million deaths in 2030.[11] Cancer can affect almost every tissue

[a]*Department of Chemistry, Quaid-i-Azam University, Islamabad-45320, Pakistan. E-mail: aamersaeed@yahoo.com; Fax: +92-51-9064-2241; Tel: +92-51-9064-2128*

[b]*Centre for Advanced Drug Research, COMSATS Institute of Information Technology, Abbottabad-22060, Pakistan. E-mail: drjamshed@ciit.net.pk*

[c]*Florida Center for Heterocyclic Compounds, Department of Chemistry, University of Florida, Fl. 32611, USA*

[d]*Center for Computationally Assisted Science and Technology, North Dakota State University, Fargo, ND, 58102, USA*

† Electronic supplementary information (ESI) available. See DOI: 10.1039/c5ra14900b

lineage in the human body and poses great challenges to medical science. Most cancers are characterized by uncontrolled cell proliferation, lack of cell differentiation and loss of contact inhibition, which confers upon the tumor cell a capability to invade local tissues and metastasize.[12,13] Nearly all cancers are caused by abnormalities in the genetic material of the transformed cells and involve deregulation of essential enzymes and other proteins controlling cell division and proliferation.[14] Many efforts have been made to the discovery of new anticancer agents which is of a paramount importance.

Over three billion people are estimated to be at risk for the parasitic diseases such as malaria, trypanosomiasis and leishmaniasis.[15] Leishmaniasis is a widespread parasitic disease that is caused by protozoan parasites of the genus *Leishmania* in tropical and subtropical areas in both the old and new worlds. According to recent World Health Organization reports, 88 countries are affected, comprehending 12 million infected people worldwide, with approximately 350 million people at risk. The incidence is increasing worldwide, with 1–2 million new cases registered annually, despite all efforts being made to fight the disease.[15–18] It occurs in three major forms; cutaneous (CL), muco-cutaneous (MCL) and visceral leishmaniasis (VL), depending upon parasite species. *L. donovani* and *L. infantum* are major causative agents of VL, while *L. major*, *L. tropica*, *L. aethiopica*, *L. braziliensis*, *L. panamensis*, *L. amazonensis* and *L. mexicana* cause CL.[19] *L. braziliensis* and *L. panamensis* are also agents of muco-cutaneous leishmaniasis. Therapy of patients with leishmaniasis is still a serious problem and urgent and sustained efforts are needed for the development of new, efficient, and safe drugs.

Heterocycles occupy a central position in organic chemistry[20–22] and are an integral part of the chemical and life sciences. Heterocyclic ring systems have emerged as powerful scaffolds for many biological evaluations playing an important role in the design and discovery of new physiological/pharmacologically active molecules.[23] Among them, 1,3-thiazole is an important and versatile structural analogue possessing a diverse spectrum of biological actions.[24–30] On the other hand, as a fragrant compound, coumarin derivatives are known to possess multiple biological functions, including anti-HIV, anti-acetylcholinesterase, antifungal, antioxidant, antihelmintic, antitumor, antibacterial, antiviral, anticancer, and anticlotting activities, and find extensive application in pharmaceuticals and agrochemicals.[31–35]

The molecular hybridization strategy involving the integration of two or more pharmacophoric units in the same

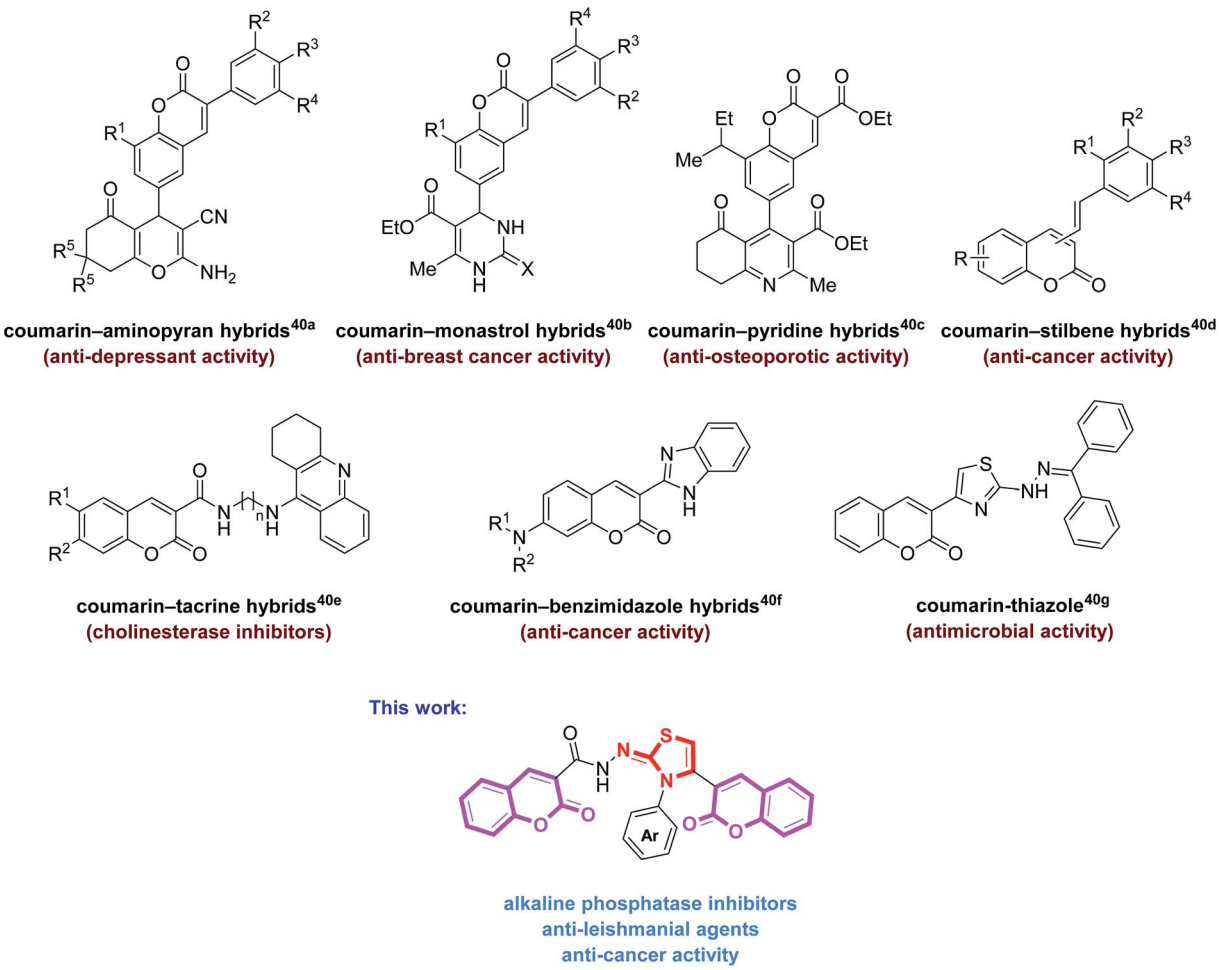

Fig. 1 Examples of bioactive coumarin-hybrid motifs and our designed hybrid molecules.

molecule, is a rationally attractive approach for the design and development of new bioactive agents.[36,37] These combined pharmacophores probably offer some advantages such as in overcoming drug resistance[38] as well as improving their biological potency.[39] The literature survey revealed the biological importance of coumarin-hybrid compounds associated with an array of biological functions. These molecules possess coumarin and other heterocyclic and non-heterocyclic skeletons (Fig. 1).[40] In view of literature findings and our continued interest aiming at developing new molecules as potent biological candidates,[31,41,42] we designed and synthesized a new series of bis-coumarin–iminothiazole hybrids using molecular hybridization approach. The synthesized compounds were evaluated for their alkaline phosphatase inhibition, anticancer and antileishmanial potential. In addition, molecular docking studies of these compounds have also been carried out to gain further insights into the biological properties. The results of this study are presented in this paper.

Results and discussion

Synthesis and characterization of bis-coumarin–iminothiazole hybrids

The reaction sequence employed for the synthesis of bis-coumarin–iminothiazole compounds (**5a–m**) is illustrated in Scheme 1. To a cold mixture of salicylaldehyde (**1**) and ethyl acetoacetate (**2**) was added catalytic amount of piperidine. The reaction mixture was stirred for 30 min at room temperature. The precipitated solid was filtered off and recrystallized (chloroform) to afford 3-acetyl-2*H*-chromen-2-one in good yield.[43] The formation of 3-acetyl-2*H*-chromen-2-one was indicated by its IR spectrum where absorption bands observed at 1759 and 1705 cm^{-1} were attributed to the C=O of ketone and lactone functionalities. ^1H NMR spectral data exhibited resonance for characteristic coumarin proton (H-4) at 8.66 ppm along with other aromatic protons at appropriate chemical shift values. Methyl protons were also observed as singlet at 2.10 ppm. 3-Acetyl-2*H*-chromen-2-one was also confirmed by ^{13}C NMR data where characteristic carbonyl carbon (ketone) appeared at 197.3 ppm in addition to lactonic carbon resonating at 156.6 ppm.

3-Acetyl-2*H*-chromen-2-one was brominated by refluxing with Br_2 solution in chloroform.[40] FTIR spectral data indicated the formation of compound (**3**) where stretching absorptions appeared at 1743 and 1716 cm^{-1} for ester and ketone carbonyls. ^1H NMR exhibited characteristic signal for methylene carbon as singlet at 4.90 ppm. Furthermore, ^{13}C NMR also confirmed the bromination of acetyl coumarin as methylene carbon resonated at 55.4 ppm.

Reaction of 3-(2-bromoacetyl)-2*H*-chromen-2-one (**3**) and substituted thiosemicarbazides (**4a–m**), synthesized previously,[31] in methanol under basic conditions afforded title products (**5a–m**) in pleasing yields.[44] The structural diversity on this scaffold was ensured by using a range of electron-rich and electron-deficient functional groups, attached to the thiazole core. The formation of thiazole derivatives (**5a–m**) was evidenced by IR spectroscopy where characteristic stretching absorptions observed in the range of 3410–3293 and 1629–1607 cm^{-1} were due to N–H and C=N groups, respectively. In ^1H NMR spectra, these compounds showed dominant signals in the range of 11.90–10.98 ppm, assigned to N–H moiety. ^{13}C NMR spectra also confirmed the presence of C=N group in the range of 159.7–157.2 ppm. The purity of the synthesized products (**5a–m**) was ascertained by elemental analysis.

Pharmacology

Alkaline phosphatase inhibition. The newly synthesized bis-coumarin–iminothiazole hybrid compounds (**5a–m**) were assayed for their alkaline phosphatase inhibition using

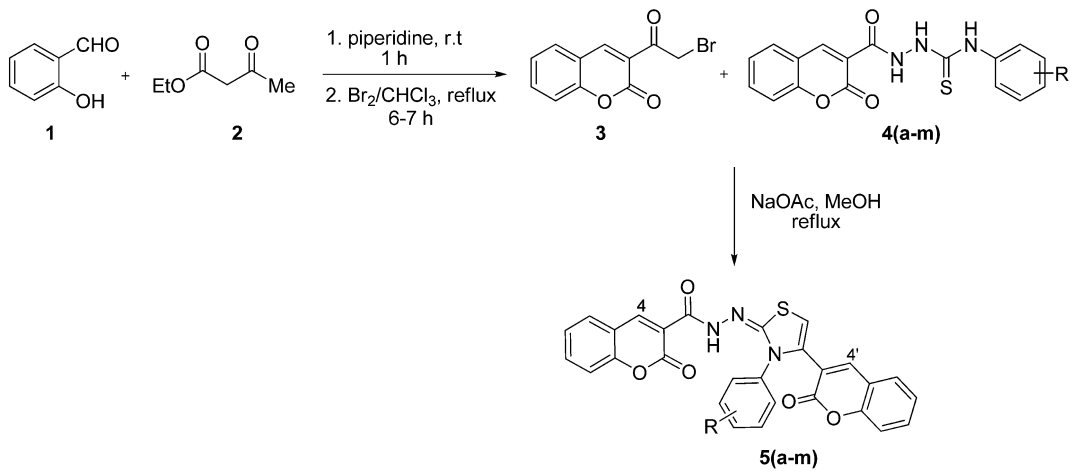

5a: R = 2-Cl; **5b:** R = 3-Cl; **5c:** R = 4-Cl; **5d:** R = 2-OMe; **5e:** R = 3-OMe; **5f:** R = 2-Me; **5g:** R = 3-Me; **5h:** R = 4-Me; **5i:** R = 2,3-diMe; **5j:** R = 2,4-diMe; **5k:** R = 2,6-diMe; **5l:** R = 3,4-diMe; **5m:** R = 3,5-diMe

Scheme 1 Synthesis of bis-coumarin–iminothiazole hybrid compounds (**5a–m**).

Table 1 Alkaline phosphatase inhibition of bis-coumarin–iminothiazole hybrids

Entry	Substituent (R)	ALP inhibition $IC_{50} \pm SEM$ (μM)
5c	4-Cl	5.78 ± 0.92
5d	2-OMe	3.92 ± 0.79
5e	3-OMe	4.36 ± 0.83
5f	2-Me	3.62 ± 0.65
5g	3-Me	4.38 ± 0.72
5h	4-Me	3.47 ± 0.67
5i	2,3-diMe	2.59 ± 0.33
5j	2,4-diMe	1.38 ± 0.42
5k	2,6-diMe	1.79 ± 0.27
5l	3,4-diMe	1.39 ± 0.21
5m	3,5-diMe	1.41 ± 0.19
KH_2PO_4	—	2.43 ± 0.04

potassium dihydrogen phosphate as standard drug (IC_{50} = 2.43 ± 0.04 μM).[45] The activity results are summarized in Table 1. The careful observation of the bioactivity results revealed that several compounds possess potent alkaline phosphatase inhibitory activity, more than the standard inhibitor.

Among the tested thiazole analogues, compound **5j** with an IC_{50} value of 1.38 ± 0.42 μM emerged as the most active compound of the series. This two-fold strong inhibitory activity may be attributed to the two methyl groups present at 3- and 5-position of aryl ring directly attached to the thiazole core. A slight modification in substituent pattern on aryl ring gave compound **5l** where substituents were present at 3- and 4-position. This compound also exhibits strong inhibitory activity (IC_{50} = 1.39 ± 0.21 μM) as compared to the standard drug. Moreover, a similar inhibitory potential was observed when methyl groups shift to 3- and 5-position at the aromatic ring as depicted by compound **5m** (IC_{50} = 1.41 ± 0.19 μM). Compound **5k** with methyl groups at 2- and 6-position also afforded potent inhibition, higher than the standard reference. Compound with methyl groups at 2- and 3-position of the aromatic ring maintained inhibitory potential comparable to standard drug. The other compounds in the series with mono substitution at various positions of aryl ring showed diminished activities. These substitutions include electron-withdrawing as well as electron-donating groups. Overall, within the synthesized series, derivatives bearing two methyl groups at variable positions of the aromatic ring attached to iminothiazole skeleton showed remarkable inhibitory potential and indicated the influence of steric factors on the modulation of alkaline phosphatase potential.

Anti-leishmanial activity. The antileishmanial activity of novel bis-coumarin–thiazole hybrids was measured by MTT method,[46,47] and %inhibition of all the synthesized compounds at different concentrations is reported in Table 2. Amphotericin B was used as a standard drug for anti-leishmanial activity.

The careful examination of the anti-leishmanial activity results revealed that most of the compounds showed >50% inhibition whereas some of the tested iminothiazoles showed good inhibition of *Leishmania major in vitro*. Among all the compounds screened in the series, **5i** showed highest inhibition of 70.4 ± 2.2% at 100 μM, whereas amphotericin B showed 79.8% inhibition. Compound **5i** incorporates two methyl substituents on the aryl ring attached directly to thiazole ring. This compound also showed highest potential at variable concentrations. The activity was reduced when these dimethyl substituents were present at variable positions as depicted by compound **5j**. Also, compound **5g** with mono methyl substituent at *meta*-position also exhibited significant inhibition (62.7 ± 1.6 μM). Apart from these substituents, electron-rich (–OMe) as well as electron-poor (–Cl) groups were tolerated which showed moderate inhibition of *Leishmania major*. Least active compound among the series was **5c** displaying 40.6 ± 2.2% inhibition at 100 μM.

Cytotoxic activity. Antiproliferative activity of the newly synthesized bis-coumarin–thiazole compounds was measured *in vitro* at four different concentrations (100, 10, 1 and 0.1 μM) by the cell growth inhibition against kidney fibroblast (BHK-21) and lung carcinoma (H-157) cell lines.[48] Vincristine was used as a standard drug for comparison to get percent inhibition of each compound.

Table 2 Anti-leishmanial activity of bis-coumarin–iminothiazole hybrids

		Leishmaniasis (%inhibition)			
Entry	Substituent (R)	100 μM	10 μM	1 μM	0.1 μM
5c	4-Cl	40.6 ± 2.2	34.6 ± 1.4	31.7 ± 1.6	22.4 ± 1.4
5d	2-OMe	58.3 ± 2.1	56.8 ± 1.7	50.4 ± 2.2	45.5 ± 1.4
5e	3-OMe	59.4 ± 1.5	56.3 ± 1.3	52.9 ± 1.5	49.3 ± 1.7
5f	2-Me	52.2 ± 1.7	51.9 ± 2.3	48.6 ± 1.7	41.7 ± 2.2
5g	3-Me	62.7 ± 1.6	59.4 ± 1.2	56.3 ± 1.4	53.7 ± 1.2
5h	4-Me	59.0 ± 1.4	57.2 ± 2.1	54.1 ± 1.6	38.2 ± 1.3
5i	2,3-diMe	70.4 ± 2.2	66.2 ± 1.4	60.7 ± 1.5	53.9 ± 1.6
5j	2,4-diMe	60.6 ± 1.5	58.7 ± 1.5	54.4 ± 1.1	52.8 ± 1.7
5k	2,6-diMe	58.4 ± 1.4	56.2 ± 1.4	49.1 ± 1.7	43.2 ± 1.1
5l	3,4-diMe	53.2 ± 1.2	47.9 ± 3.7	43.2 ± 2.2	38.6 ± 1.3
5m	3,5-diMe	53.8 ± 2.1	49.7 ± 1.2	45.3 ± 1.3	36.4 ± 1.2
Amphotericin B	—	79.8 ± 1.8	76.3 ± 1.4	74.8 ± 2.7	69.9 ± 2.3

Most of the compounds among thiazole series exhibited (>50%) inhibition for both cell lines with slightly different capacity due to their structure diversity in terms of attached functional groups with thiazole skeleton (Tables 3 and 4). Among the tested compounds, **5m** showed the highest inhibition of 66.8 ± 1.1 and 64.2 ± 2.3% at 100 and 10 μM, respectively, against BHK-21 cells. This compound possesses dimethyl substituent at 3- and 5-position of the aryl ring at thiazole skeleton. A slight decrease in inhibition was observed when substitution pattern is changed to 2,4- or 3,4-positions as depicted by compound **5j** and **5l**, respectively. Several other substitutions including electron-donating and electron-withdrawing were also tolerated but afforded reduced inhibition. Compound **5k** bearing dimethyl substitution at 2- and 6-position gave least inhibition of 37.8 ± 1.2% at 0.1 μM concentration. Compounds with only one methyl group at *ortho*- or *para*-position exhibited inhibition slightly greater than 50% at 100 and 10 μM.

In case of H-157 cell lines, among the tested thiazole hybrids, compound **5l** was the most potent analogue with inhibition value of 65.0 ± 1.8% at 100 μM while 57.3 ± 0.7% at 10 μM. This activity may be attributed to the presence of dimethyl groups at 3- and 4-position of aryl ring attached to thiazole core. A slight downward shift in activity was observed when position of substituents is moved to 2- and 4-position or 3- and 5-position, respectively. Compounds **5j** and **5m** with dimethyl substituents at 2- and 4-position and 3- and 5-position showed 61.4 ± 1.6 and 61.1 ± 1.2% inhibitions at 10 μM, respectively as compared to vincristine (72.6 ± 3.1% at 10 μM). Least activity was observed in case of **5g** which incorporates only one methyl group at *meta*-position.

In general, among the tested bis-coumarin–iminothiazole hybrids, the compounds with dual substitutions were found to possess highest activities and emerged as lead candidates. This pattern also suggests that the steric factors are generally more operative in modulating the activity profile as compared to the electronic properties. These results also speculate some further research to optimize bis-coumarin–iminothiazole template against a range of biological targets with promising inhibitory potential.

Molecular modelling

Druglikeness, Lipinski's rule of five. Molecular descriptors were calculated for all the synthesized compounds by the ligand

Table 3 Anticancer activity of bis-coumarin–iminothiazole hybrids against kidney fibroblast (BHK-21) cell lines

		BHK-21 cell lines (%inhibition)			
Entry	Substituent (R)	100 μM	10 μM	1 μM	0.1 μM
5c	4-Cl	50.5 ± 1.4	48.3 ± 1.2	47.2 ± 1.8	41.8 ± 2.5
5d	2-OMe	59.4 ± 1.3	55.3 ± 1.7	52.8 ± 1.2	47.0 ± 1.7
5e	3-OMe	53.2 ± 1.7	50.2 ± 2.1	46.3 ± 1.8	45.5 ± 1.2
5f	2-Me	54.7 ± 1.2	51.8 ± 2.4	49.9 ± 1.6	47.2 ± 1.6
5g	3-Me	52.9 ± 1.3	50.7 ± 1.5	47.3 ± 2.3	45.1 ± 1.8
5h	4-Me	57.3 ± 1.5	54.8 ± 2.8	50.5 ± 1.7	48.7 ± 1.2
5i	2,3-diMe	57.2 ± 1.2	51.6 ± 2.5	47.2 ± 2.6	41.9 ± 3.3
5j	2,4-diMe	62.9 ± 3.2	61.1 ± 2.6	60.7 ± 1.8	56.4 ± 2.4
5k	2,6-diMe	54.7 ± 2.1	51.8 ± 2.4	44.3 ± 2.7	37.8 ± 1.2
5l	3,4-diMe	62.1 ± 1.8	61.8 ± 1.2	56.4 ± 2.9	52.9 ± 1.9
5m	3,5-diMe	66.8 ± 1.1	64.2 ± 2.3	59.4 ± 1.2	55.5 ± 2.7
Vincristine	—	74.5 ± 2.9	72.6 ± 3.1	70.9 ± 2.4	69.8 ± 1.9

Table 4 Anticancer activity of bis-coumarin–iminothiazole hybrids against lung carcinoma (H-157) cell lines

		H-157 cell lines (%inhibition)			
Entry	Substituent (R)	100 μM	10 μM	1 μM	0.1 μM
5c	4-Cl	53.7 ± 1.6	50.3 ± 0.8	47.2 ± 2.7	44.7 ± 1.2
5d	2-OMe	54.4 ± 1.5	52.3 ± 1.3	49.4 ± 1.7	48.4 ± 1.2
5e	3-OMe	52.5 ± 0.7	49.8 ± 1.1	44.9 ± 1.2	35.2 ± 1.6
5f	2-Me	56.6 ± 1.4	52.4 ± 1.9	47.5 ± 2.8	44.3 ± 2.7
5g	3-Me	51.0 ± 1.3	44.2 ± 2.5	38.1 ± 2.4	32.8 ± 1.3
5h	4-Me	54.6 ± 1.8	51.8 ± 2.7	50.9 ± 1.1	47.6 ± 1.5
5i	2,3-diMe	54.4 ± 3.9	51.7 ± 1.7	47.2 ± 1.2	43.6 ± 1.3
5j	2,4-diMe	63.6 ± 2.0	61.4 ± 1.6	56.7 ± 2.4	52.1 ± 1.4
5k	2,6-diMe	57.9 ± 1.1	55.2 ± 0.4	51.6 ± 1.1	44.4 ± 1.6
5l	3,4-diMe	65.0 ± 1.8	57.3 ± 0.7	53.8 ± 2.6	45.5 ± 1.7
5m	3,5-diMe	63.0 ± 3.1	61.1 ± 1.2	57.4 ± 2.1	54.3 ± 2.5
Vincristine	—	74.5 ± 2.9	72.6 ± 3.1	70.9 ± 2.4	69.8 ± 1.9

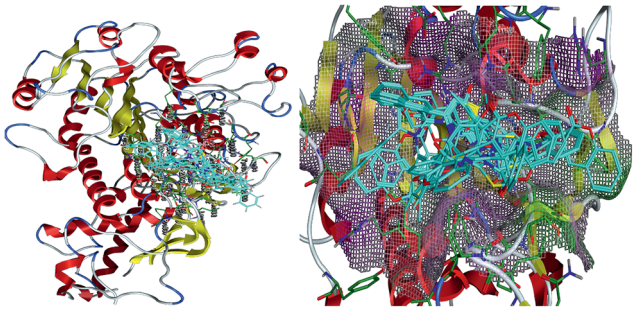

Fig. 2 Superimposition of the ligands inside the active site; (a) overlaying of all the minimum energy docked poses inside the pocket. Ligands are shown in cyan color in stick mode while key residues are shown in green color in stick mode. Backbone receptor is shown in cartoon and ribbon form. (b) Close view of the active site, pocket is marked with surfaces.

property calculation function of MOE (Table S1†) and all of them were found to obey Lipinski's Ro5 and Veber's Ro3, cut-off limits,[49,50] revealing the fact that these could be potent alkaline phosphatase inhibitors.

According to Lipinski's Ro5, most drug like molecules have molecular weight $\leq$ 500, logarithm of the octanol/water partition coefficient (log P) $\leq$ 5, total polar surface area (TPSA) < 140 Å^2, number of hydrogen bond donors (HBD) $\leq$ 5 and hydrogen bond acceptor (HBA) $\leq$ 10.[50] Further modifications in the Ro5 were made by Veber *et al.*[49] who suggested the number of rotatable bond (NOR) of drug like molecule must be fewer or equal to 10.[50] Molecules violating more than one of these rules may have problem with bioavailability.

Docking studies. For elucidation of the molecular mechanism of inhibition of the synthesized library of imino-thiazole derivatives, compounds were docked computationally to the active site of alkaline phosphatase (ALP) from rat (PDB code: 4KJG).[51]

Structural analyses of the 3D generated model of the ALP showed that enzyme is constructed with two chains with the co-crystallized ligand in each chain, pocket was found around the co-crystallized ligand. After docking the standard drug in the pocket of both chains, the active site of the chain B was selected for further studies. Pocket was found to be a small cavity, mostly constructed with hydrophilic residues some of these are Tyr107, Lys108, Arg166, His153, Val89, His 320, Ser429, Thr431 and Gln317. Molecular docking studies were carried out to determine the probable binding modes of these compounds in the active sites of the enzyme, rat Intestinal Alkaline Phosphate (IALP) (PDB code: 4KJG). All the docked conformations of each ligands were analyzed. From the results of calculations, we chose variants with the minimal energy of the enzyme–inhibitor complex. All the preferred docked conformations formed one cluster inside the pocket as shown in Fig. 2.

Almost all the compounds have similar binding interaction pattern. In all the ligands except **5c**, **5f**, **5h**, **5i** and **5m**, the carbonyl oxygen present on the coumarin moiety formulated strong hydrogen bonding with the amino acid residues in active site, while phenyl ring of the same moiety established H–arene interaction in all the ligands except **5d** and **5k**. In addition to these, tremendous polar interactions also played important role for strong binding of the ligands inside the active site. Compounds **5j–m** are found to be the most active compounds of the series and these compounds were also found to exhibit strong interaction with the amino acids residues inside the active site. Compound **5m** inhibited the catalytic activities of the ALP by anchoring over active site through multiple polar interactions, a hydrophobic interaction and Pi–H interaction although it didn't establish hydrogen bonding like other three most active compounds **5j**, **5k** and **5l**. Fig. 3 shows plausible binding modes for three most active representative compounds **5j**, **5k** and **5l** of the series. While images of 2D interaction for all the ligands along with the detailed legend are shown in Fig. S1.† The binding free energies derived from docking (London dG ranging from −11.4376 to −7.4100 kcal mol^{-1}) indicate that almost all the synthesized imino-thiazole derivatives exhibited stronger binding affinity for alkaline phosphatase (Table S2†). The poses are ranked by the scores from the GBVI/WSA binding free energy calculation in the "S" field. It is quite interesting to note that the binding free energy in "S" field is in quite narrow range from −6.0532 to −6.8090 kcal mol^{-1} (Table S2†). According to the computations performed, all the docked ligands are located in the active site of alkaline phosphatase (PDB code: 4KJG).[51] Investigation of the binding mode analysis of the adopted conformations revealed that both the phenyl rings (coumarin moiety) are oriented almost in parallel to the main plane. This orientation of phenyl rings may lead to its interaction (H–arene) with the amino acid residues in the active site of alkaline phosphatase.

The calculated geometries of the inhibitor **5l** in the enzyme's active site was analyzed to study the orientation of its docking pose and binding mode as shown in Fig. 4. As a result the positions of oxygen, it formed a strong H-bonding with the Asp167, His153 and Lys108 in addition to H–arene interaction of the phenyl ring with His432. Several strong polar interactions may reflect additional fixation of inhibitor **5l** which occupied the enzyme's active site. Again binding of two phenyl rings through Pi–H interaction with key residues could be the strong reason of low energy and good activity of the inhibitor **5l** (Fig. 3c and 4). Examination of the most preferred docked pose of inhibitor **5k** (Fig. 3b) revealed that the oxygen atom of the carbonyl group established a strong hydrogen bond with Lys108. In addition to these, several polar interactions also played a significant role for strong binding, low binding energy and in turn good activity of the entire imino-thiazole library against ALP. The synthesized library **5a–m** is composed basically of three phenyl rings, causing the whole structure to be quite rigid and bulky. The rigidity imparted the expanded orientation to the compounds which favored the maximum exposure of the ligand to active site residues leading to remarkable interactions.

It can be concluded from the docking computations that quite low binding free energy (−6.0532 to −6.8090 kcal mol^{-1}) coupled with the multiple interactions with amino acids residues provided the rational for good activities of these inhibitors specially **5j–m** (IC_{50} = 1.38 to 1.79 μM) which were noticed to be

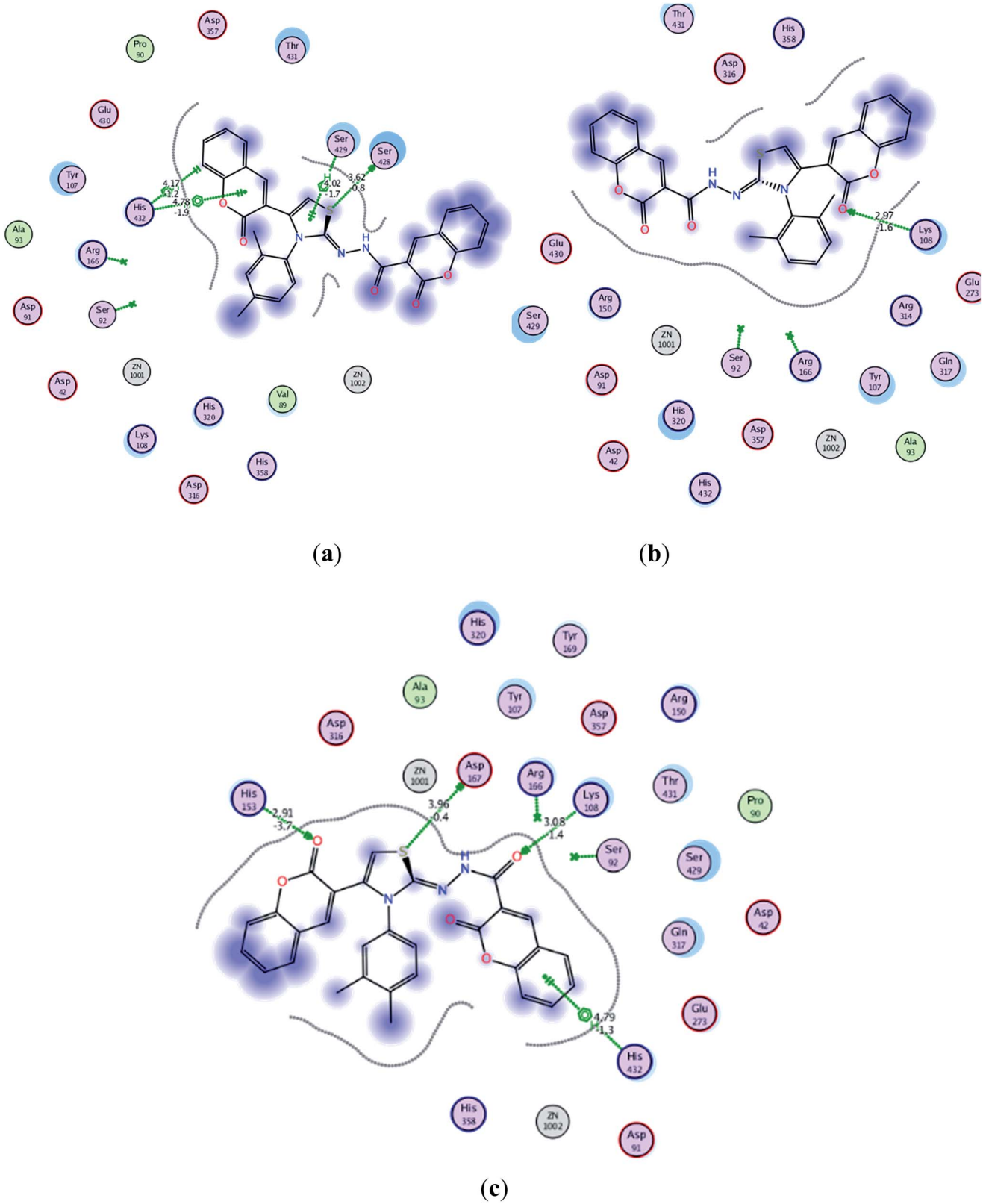

Fig. 3 Interaction of ligands with the active site residues of receptor in 2D space; dotted green lines present hydrogen bonding and other interactions. Detailed description is given in the Fig. S1 in ESI† under the caption legend (a) compound **5j** (b) compound **5k** and (c) compound **5l**.

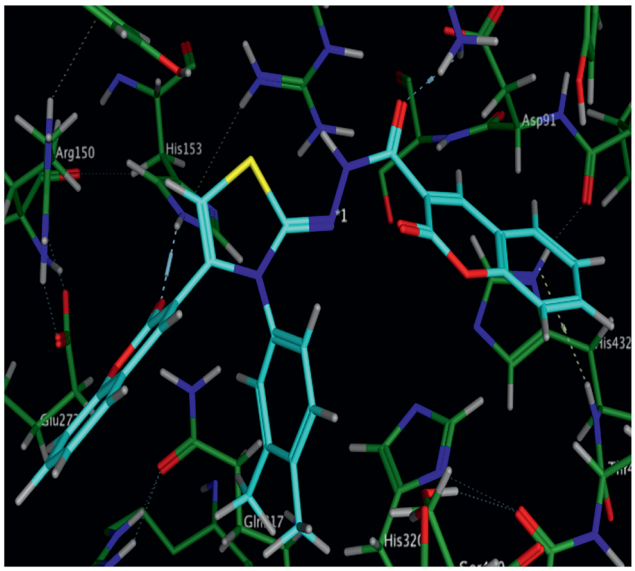

Fig. 4 Docking pose of the ligand **5l** inside the active site. Interaction of ligand **5l** with the active site residues of receptor in 3D space; dashed blue lines represent hydrogen bonding while dotted yellow line represents H–arene interaction.

more potent as compared to standard drug (IC_{50} = 2.43 μM) against IALP. This is in accordance with findings that introducing coumarin moieties at the both terminal of the structure of thiazoles lead to greater strength in addition to imparting the flat, expanded orientation to the structures which consequently helped in strong binding. This can provide the rational for more effective binding through hydrogen bonding and arene–H interaction in the enzyme active site. These results proclaimed compounds **5j–m** to be further developed as ALP inhibitors.

Conclusions

In summary, a series of novel bis-coumarin–iminothiazole hybrids (**5a–m**) has been prepared by the reaction of bromoacetyl coumarin and a range of thiosemicarbazide derivatives in methanol. The structural diversity of the synthesized derivatives was ensured by using a diverse range of substituents including electron-donating and electron-withdrawing groups on aryl part of thiosemicarbazide. The synthesized analogues were screened against alkaline phosphatase where **5j** emerged as a potent inhibitor with an IC_{50} value of 1.38 ± 0.42 μM which is two-fold strong inhibition as compared to the standard inhibitor. The synthesized compounds were also assayed for their anti-leishmanial potential and compound **5i** was found to be the lead candidate with 70.4 ± 2.2% inhibition at 100 μM. The prepared compounds also showed cytotoxic behavior against kidney fibroblast (BHK-21) and lung carcinoma (H-157) cell lines. Compound **5l** showed dual inhibition (66.8 ± 1.1 and 65.0 ± 1.8%) against BHK-21 and H-157 cell lines, respectively. In general, among the tested bis-coumarin–iminothiazole hybrids, the compounds with dual substitutions were found to possess highest activities and emerged as lead candidates. This pattern also suggests that the steric factors are generally more operative in modulating the activity profile as compared to the electronic properties. The detailed binding mode analysis with docking simulation showed that the inhibitors could be stabilized in the active site through the formation of multiple interactions with catalytic residues and the establishment of hydrophobic contacts in a cooperative fashion. Finally, based on the activity findings and docking analysis, it could be proclaimed that the synthesized inhibitors could be further developed as novel and potent inhibitors of alkaline phosphatase.

Experimental

General

Unless otherwise noted, all materials were obtained from commercial suppliers (Aldrich and Merck companies) and used without further purification. Thin layer chromatography (TLC) was performed on Merck DF-Alufoilien $60F_{254}$ 0.2 mm precoated plates. Product spots were visualized under UV light at 254 and 365 nm. Melting points were recorded on a Stuart melting point apparatus (SMP3) and are uncorrected. Infra-red (IR) spectra were recorded on FTS 3000 MX, Bio-Rad Merlin (Excalibur model) spectrophotometer. ^{1}H NMR spectra were recorded on a Bruker Avance (300 MHz) spectrometer. Chemical shifts (δ) are quoted in parts per million (ppm) downfield of tetramethylsilane, using residual solvent as internal standard (DMSO-d_6 at 2.50 ppm). Abbreviations used in the description of resonances are: s (singlet), d (doublet), t (triplet), q (quartet), m (multiplet), Ar (aromatic). Proton-decoupled ^{13}C NMR spectra were recorded on a Bruker Avance (75 MHz) spectrometer using deuterated solvent as internal standard (DMSO-d_6 at 39.52 ppm). The elemental analysis was performed on Leco CHNS-932 Elemental Analyzer, Leco Corporation (USA).

Synthesis of 3-acetyl-2*H*-chromen-2-one

To a cold mixture of salicylaldehyde **1** (1.0 mol) and ethyl acetoacetate **2** (1.0 mol), catalytic amount of piperidine was added and reaction mixture was stirred for 30 min at room temperature. The solid separated was filtered and washed with ethanol. Recrystallization of the solid from chloroform afforded 3-acetyl-2*H*-chromene-2-one.[43] Yield (93%): m.p.: 119–121 °C; R_f: 0.61 (20% EtOAc/hexane). The data for 3-acetyl-2*H*-chromene-2-one was consistent with literature.[52]

Synthesis of 3-(2-bromoacetyl)-2*H*-chromen-2-one (3)

3-Acetyl-2*H*-chromene-2-one (10.0 mmol) was dissolved in dry chloroform and a solution of Br_2 (10.0 mmol) in chloroform was added dropwise with continuous stirring and mixture was heated at reflux for 6–7 h. The progress of the reaction was monitored by thin layer chromatography (TLC). After completion of the reaction, the mixture was concentrated under reduced pressure, and washed with diethyl ether and recrystallized (70% $CHCl_3$/EtOH) to afford 3-(2-bromoacetyl)-2*H*-chromen-2-one (**3**).[40] Yield: (69%); m.p.: 161–163 °C; R_f: 0.26 (20% EtOAc/hexane). The data for **3** was consistent with those observed in the literature.[52]

Synthesis of 1,4-disubstituted thiosemicarbazides (4a–m)

The carbohydrazide (6.8 mmol) was dissolved in methanol (30 mL), and a solution of substituted isothiocyanate (6.6 mmol) separately dissolved in methanol (10 mL) was added dropwise with continuous stirring. The reaction mixture was heated at reflux for 10–12 h and monitored by TLC. After consumption of the starting materials, the mixture was cooled to room temperature. The methanol was evaporated under reduced pressure leaving behind the crude product as oil that became solidified on cooling and was recrystallized (20% EtOAc/hexane) to yield thiosemicarbazides (**4a–m**).[31] The spectroscopic data for thiosemicarbazides (**4a–h**) has previously been reported in our papers[31] (R_f = 20% EtOAc/hexane).

***N*-(2,3-Dimethylphenyl)-2-(2-oxo-2*H*-chromene-3-carbonyl)-hydrazinecarbothioamide (4i).** Yield: (59%); m.p.: 171–173 °C; R_f: 0.51; IR (ATR, cm^{-1}): 3464–3223 (NH), 1717 (C=O), 1572, 1540 (C=C), 1271 (C=S); ^{1}H NMR (300 MHz, DMSO-d_6): δ 11.51 (s, 1H, NH–C=O), 11.13 (s, 2H, NH–C=S), 9.01 (s, 1H, H-4), 7.71–7.68 (m, 2H, ArH), 7.43–7.38 (m, 1H, ArH), 7.27–7.17 (m, 1H, ArH), 7.00–6.95 (m, 2H, ArH), 6.16–6.13 (m, 1H, ArH), 2.27 (s, 3H, CH_3), 2.09 (s, 3H, CH_3); ^{13}C NMR (75 MHz, DMSO-d_6): δ 177.3, 164.4, 159.8, 152.7, 140.1, 136.9, 133.3, 130.8, 127.4, 125.1, 123.5, 120.7, 119.0, 117.3, 116.3, 114.1, 112.7, 22.2, 17.3; anal. calcd for $C_{19}H_{17}N_3O_3S$: C, 62.10; H, 4.64; N, 11.43; S, 8.71; found: C, 62.02; H, 4.58; N, 11.39; S, 8.65.

***N*-(2,4-Dimethylphenyl)-2-(2-oxo-2*H*-chromene-3-carbonyl)-hydrazinecarbothioamide (4j).** Yield: (68%); m.p.: 166–168 °C; R_f: 0.53; IR (ATR, cm^{-1}): 3392–3263 (NH), 1716 (C=O), 1569, 1528 (C=C), 1269 (C=S); ^{1}H NMR (300 MHz, DMSO-d_6): δ 11.54 (s, 1H, NH–C=O), 11.10 (s, 2H, NH–C=S), 9.13 (s, 1H, H-4), 7.73–7.69 (m, 2H, ArH), 7.43–7.40 (m, 2H, ArH), 6.97–6.95 (m, 1H, ArH), 6.67–6.63 (m, 1H, ArH), 6.13–6.11 (m, 1H, ArH), 2.27 (s, 3H, CH_3), 2.02 (s, 3H, CH_3); ^{13}C NMR (75 MHz, DMSO-d_6): δ 178.0, 163.1, 159.8, 153.1, 143.3, 139.0, 132.3, 130.7, 129.1, 127.3, 126.1, 122.6, 120.3, 119.6, 118.2, 116.1, 114.3, 21.3, 17.8; anal. calcd for $C_{19}H_{17}N_3O_3S$: C, 62.10; H, 4.59; N, 11.40; S, 8.69; found: C, 62.03; H, 4.51; N, 11.31; S, 8.63.

***N*-(2,6-Dimethylphenyl)-2-(2-oxo-2*H*-chromene-3-carbonyl)-hydrazinecarbothioamide (4k).** Yield: (66%); m.p.: 161–163 °C; R_f: 0.51; IR (ATR, cm^{-1}): 3442–3293 (NH), 1712 (C=O), 1572, 1523 (C=C), 1269 (C=S); ^{1}H NMR (300 MHz, DMSO-d_6): δ 11.43 (s, 1H, NH–C=O), 11.02 (s, 2H, NH–C=S), 9.09 (s, 1H, H-4), 7.78–7.70 (m, 2H, ArH), 7.45–7.43 (m, 2H, ArH), 6.95–6.92 (m, 2H, ArH), 6.63–6.61 (m, 1H, ArH), 2.19 (s, 6H, CH_3); ^{13}C NMR (75 MHz, DMSO-d_6): δ 171.1, 161.9, 158.2, 153.0, 141.1, 138.4, 133.0, 128.1, 127.0, 125.1, 123.7, 121.0, 119.3, 116.7, 114.2, 23.9; anal. calcd for $C_{19}H_{17}N_3O_3S$: C, 62.09; H, 4.60; N, 11.39; S, 8.68; found: C, 62.01; H, 4.54; N, 11.35; S, 8.61.

***N*-(3,4-Dimethylphenyl)-2-(2-oxo-2*H*-chromene-3-carbonyl)-hydrazinecarbothioamide (4l).** Yield: (55%); m.p.: 164–166 °C; R_f: 0.56; IR (ATR, cm^{-1}): 3453–3343 (NH), 1720 (C=O), 1565, 1549 (C=C), 1263 (C=S); ^{1}H NMR (300 MHz, DMSO-d_6): δ 11.63 (s, 1H, NH–C=O), 11.11 (s, 2H, NH–C=S), 8.86 (s, 1H, H-4), 7.73–7.65 (m, 2H, ArH), 7.42–7.41 (m, 2H, ArH), 6.86 (m, 1H, ArH), 6.23–6.21 (m, 2H, ArH), 2.36 (s, 3H, CH_3), 2.27 (s, 3H, CH_3); ^{13}C NMR (75 MHz, DMSO-d_6): δ 179.2, 163.9, 158.4, 152.2, 144.0, 139.8, 135.7, 133.8, 131.0, 129.3, 127.8, 125.5, 122.4, 119.1, 117.6, 116.6, 114.7, 22.3, 19.3; anal. calcd for $C_{19}H_{17}N_3O_3S$: C, 62.11; H, 4.62; N, 11.40; S, 8.67; found: C, 62.00; H, 4.52; N, 11.37; S, 8.61.

***N*-(3,5-Dimethylphenyl)-2-(2-oxo-2*H*-chromene-3-carbonyl)-hydrazinecarbothioamide (4m).** Yield: (63%); m.p.: 160–162 °C; R_f: 0.52; IR (ATR, cm^{-1}): 3423–3281 (NH), 1708 (C=O), 1562, 1529 (C=C), 1259 (C=S); ^{1}H NMR (300 MHz, DMSO-d_6): δ 11.48 (s, 1H, NH–C=O), 11.09 (s, 2H, NH–C=S), 9.09 (s, 1H, H-4), 7.79–7.66 (m, 2H, ArH), 7.42–7.39 (m, 2H, ArH), 6.69–6.66 (m, 3H, ArH), 2.27 (s, 6H, CH_3); ^{13}C NMR (75 MHz, DMSO-d_6): δ 175.6, 163.2, 157.4, 151.2, 140.8, 137.0, 131.2, 129.6, 127.8, 124.5, 123.1, 120.2, 118.8, 115.0, 113.5, 19.9; anal calcd for $C_{19}H_{17}N_3O_3S$: C, 62.08; H, 4.59; N, 11.38; S, 8.69; found: C, 62.03; H, 4.50; N, 11.33; S, 8.59.

Synthesis of (*E*)-*N*′-(3-(substituted)-4-(2-oxo-2*H*-chromen-3-yl)-thiazol-2(3*H*)-ylidene)-2-oxo-2*H*-chromene-3-carbohydrazide (5a–m)

To a mixture of substituted thiosemicarbazide (**4a–m**) (1.0 mmol) and 3-(2-bromoacetyl)-2*H*-chromen-2-one (**3**) (1.0 mmol) in methanol, anhydrous sodium acetate (4.0 mmol) was added and heated at reflux for 5–6 h. The reaction mixture was then cooled to room temperature and the solid product formed was filtered off, washed with water, dried ($MgSO_4$), and recrystallized (EtOH) to afford title products (**5a–m**) in good yields[44] (R_f = 20% EtOAc/hexane).

(*E*)-*N*′-(3-(2-Chlorophenyl)-4-(2-oxo-2*H*-chromen-3-yl)thiazol-2(3*H*)-ylidene)-2-oxo-2*H*-chromene-3-carbohydrazide (5a). Yield: (58%); m.p.: 190–192 °C; R_f: 0.42; IR (ATR, cm^{-1}): 3329 (NH), 1717, 1703 (C=O), 1629 (C=N); ^{1}H NMR (300 MHz, DMSO-d_6): δ 11.23 (s, 1H, NH), 9.67 (s, 1H, H-4), 8.98 (s, 1H, H-4′), 7.96–7.79 (m, 4H, ArH), 7.43–7.40 (m, 5H, ArH), 7.23–7.21 (m, 1H, ArH), 7.01–6.86 (m, 2H, ArH), 6.66–6.60 (m, 1H, ArH); ^{13}C NMR (75 MHz, DMSO-d_6): δ 168.3, 159.1, 154.0, 151.2, 148.6, 143.2, 133.9, 131.6, 130.4, 129.1, 128.6, 127.3, 126.7, 125.3, 123.5, 121.2, 119.8, 118.0, 116.3, 112.5, 98.6; anal. calcd for $C_{28}H_{16}ClN_3O_5S$: C, 62.04; H, 2.96; N, 7.73; S, 5.90; found: C, 62.00; H, 2.90; N, 7.68; S, 5.87.

(*E*)-*N*′-(3-(3-Chlorophenyl)-4-(2-oxo-2*H*-chromen-3-yl)thiazol-2(3*H*)-ylidene)-2-oxo-2*H*-chromene-3-carbohydrazide (5b). Yield: (60%); m.p.: 182–184 °C; R_f: 0.46; IR (ATR, cm^{-1}): 3298 (NH), 1732, 1712 (C=O), 1619 (C=N); ^{1}H NMR (300 MHz, DMSO-d_6): δ 11.48 (s, 1H, NH), 9.89 (s, 1H, H-4), 9.01 (s, 1H, H-4′), 8.01–7.93 (m, 4H, ArH), 7.42–7.09 (m, 5H, ArH), 7.03–6.95 (m, 2H, ArH), 6.90–6.86 (m, 1H, ArH), 6.65–6.63 (m, 1H, ArH); ^{13}C NMR (75 MHz, DMSO-d_6): δ 169.1, 158.3, 153.4, 150.1, 149.6, 142.0, 135.7, 133.0, 131.8, 130.6, 128.5, 127.0, 126.4, 125.1, 122.7, 121.3, 119.6, 118.1, 116.6, 114.8, 99.1; anal. calcd for $C_{28}H_{16}ClN_3O_5S$: C, 62.04; H, 2.96; N, 7.73; S, 5.90; found: C, 62.02; H, 2.88; N, 7.70; S, 5.85.

(*E*)-*N*′-(3-(4-Chlorophenyl)-4-(2-oxo-2*H*-chromen-3-yl)thiazol-2(3*H*)-ylidene)-2-oxo-2*H*-chromene-3-carbohydrazide (5c). Yield: (66%); m.p.: 196–198 °C; R_f: 0.48; IR (ATR, cm^{-1}): 3311 (NH), 1725, 1705 (C=O), 1612 (C=N); ^{1}H NMR (300 MHz, DMSO-d_6): δ 11.48 (s, 1H, NH), 8.59 (s, 1H, H-4), 8.19 (s, 1H, H-

4′), 7.89–7.80 (m, 4H, ArH), 7.68–7.61 (m, 4H, ArH), 7.48–7.36 (m, 4H, ArH); ^{13}C NMR (75 MHz, DMSO-d_6): δ 158.8, 158.7, 155.1, 154.9, 149.2, 149.1, 147.8, 135.6, 135.1, 131.5, 131.3, 125.6, 125.5, 123.2, 122.6, 118.6, 118.5, 118.3, 116.7; anal. calcd for $C_{28}H_{16}ClN_3O_5S$: C, 62.04; H, 2.96; N, 7.73; S, 5.90; found: C, 62.00; H, 2.90; N, 7.69; S, 5.87.

(*E*)-*N*′-(3-(2-Methoxyphenyl)-4-(2-oxo-2*H*-chromen-3-yl)thiazol-2(3*H*)-ylidene)-2-oxo-2*H*-chromene-3-carbohydrazide (5d). Yield: (69%); m.p.: 174–176 °C; R_f: 0.42; IR (ATR, cm^{-1}): 3312 (NH), 1717, 1698 (C=O), 1615 (C=N); ^{1}H NMR (300 MHz, DMSO-d_6): δ 11.90 (s, 1H, NH), 8.48 (s, 1H, H-4), 8.33 (s, 1H, H-4′), 8.32–8.25 (m, 2H, ArH), 7.90 (t, J = 8.7 Hz, 1H, ArH), 7.28–7.00 (m, 3H, ArH), 6.98–6.96 (m, 3H, ArH), 6.94–6.92 (m, 2H, ArH), 6.89–6.86 (m, 3H, ArH), 3.88 (s, 3H, OCH_3); ^{13}C NMR (75 MHz, DMSO-d_6): δ 169.7, 159.2, 152.7, 147.3, 144.4, 138.4, 138.2, 136.6, 134.4, 132.1, 129.2, 128.9126.1, 125.2, 121.1, 119.6, 116.3, 113.2, 111.9, 111.5, 64.5; anal. calcd for $C_{29}H_{19}N_3O_6S$: C, 64.79; H, 3.54; N, 7.80; S, 5.96; found: C, 64.73; H, 3.49; N, 7.73; S, 5.91.

(*E*)-*N*′-(3-(3-Methoxyphenyl)-4-(2-oxo-2*H*-chromen-3-yl)thiazol-2(3*H*)-ylidene)-2-oxo-2*H*-chromene-3-carbohydrazide (5e). Yield: (62%); m.p.: 167–169 °C; R_f: 0.40; IR (ATR, cm^{-1}): 3332 (NH), 1721, 1702 (C=O), 1623 (C=N); ^{1}H NMR (300 MHz, DMSO-d_6): δ 11.67 (s, 1H, NH), 9.15 (s, 1H, H-4), 8.68 (s, 1H, H-4′), 8.38–8.27 (m, 2H, ArH), 7.73–7.62 (m, 4H, ArH), 7.30–7.26 (m, 1H, ArH), 7.10–6.99 (m, 4H, ArH), 6.38–6.31 (m, 2H, ArH), 3.65 (s, 3H, OCH_3); ^{13}C NMR (75 MHz, DMSO-d_6): δ 169.7, 159.3, 157.1, 151.6, 150.7, 148.1, 143.9, 132.0, 130.7, 128.1, 126.1, 125.2, 124.6, 123.3, 121.7, 120.3, 119.9, 116.6, 111.6, 110.7, 95.8, 56.3; anal. calcd for $C_{29}H_{19}N_3O_6S$: C, 64.79; H, 3.54; N, 7.80; S, 5.96; found: C, 64.71; H, 3.50; N, 7.70; S, 5.89.

(*E*)-2-Oxo-*N*′-(4-(2-oxo-2*H*-chromen-3-yl)-3-*o*-tolylthiazol-2(3*H*)-ylidene)-2*H*-chromene-3-carbohydrazide (5f). Yield: (67%); m.p.: 109–111 °C; R_f: 0.48; IR (ATR, cm^{-1}): 3381 (NH), 1719, 1699 (C=O), 1609 (C=N); ^{1}H NMR (300 MHz, DMSO-d_6): δ 11.70 (s, 1H, NH), 8.47 (s, 1H, H-4), 8.10 (s, 1H, H-4′), 7.43–7.41 (m, 4H, ArH), 7.26–7.14 (m, 4H, ArH), 7.00–6.81 (m, 4H, ArH), 2.30 (s, 3H, CH_3); ^{13}C NMR (75 MHz, DMSO-d_6): δ 167.2, 153.0, 149.6, 146.2, 144.8, 138.9, 137.0, 134.8, 131.7, 128.9, 127.5, 126.2, 120.7, 119.6, 116.4, 115.7, 114.6, 111.4, 21.0; anal. calcd for $C_{29}H_{19}N_3O_5S$: C, 66.77; H, 3.67; N, 8.05; S, 6.13; found: C, 66.68; H, 3.60; N, 8.01; S, 6.08.

(*E*)-2-Oxo-*N*′-(4-(2-oxo-2*H*-chromen-3-yl)-3-*m*-tolylthiazol-2(3*H*)-ylidene)-2*H*-chromene-3-carbohydrazide (5g). Yield: (63%); m.p.: 113–115 °C; R_f: 0.47; IR (ATR, cm^{-1}): 3398 (NH), 1716, 1705 (C=O), 1616 (C=N); ^{1}H NMR (300 MHz, DMSO-d_6): δ 11.21 (s, 1H, NH), 9.43 (s, 1H, H-4), 8.86 (s, 1H, H-4′), 7.86–7.79 (m, 4H, ArH), 7.53–7.35 (m, 5H, ArH), 7.03–6.98 (m, 2H, ArH), 6.66–6.60 (m, 1H, ArH), 6.53–6.49 (m, 1H, ArH), 2.12 (s, 3H, CH_3); ^{13}C NMR (75 MHz, DMSO-d_6): δ 169.1, 158.3, 153.6, 151.2, 148.5, 137.2, 132.9, 131.2, 129.1, 128.6, 127.1, 126.0, 124.7, 122.5, 121.7, 119.2, 117.6, 116.1, 114.3, 111.5, 98.7, 20.1; anal. calcd for $C_{29}H_{19}N_3O_5S$: C, 66.77; H, 3.67; N, 8.05; S, 6.13; found: C, 66.70; H, 3.62; N, 8.00; S, 6.06.

(*E*)-2-Oxo-*N*′-(4-(2-oxo-2*H*-chromen-3-yl)-3-*p*-tolylthiazol-2(3*H*)-ylidene)-2*H*-chromene-3-carbohydrazide (5h). Yield: (68%); m.p.: 108–110 °C; R_f: 0.49; IR (ATR, cm^{-1}): 3410 (NH), 1725, 1707 (C=O), 1607 (C=N); ^{1}H NMR (300 MHz, DMSO-d_6): δ 11.09 (s, 1H, NH), 9.68 (s, 1H, H-4), 8.94 (s, 1H, H-4′), 7.98–7.84 (m, 4H, ArH), 7.65–7.62 (m, 2H, ArH), 7.46–7.39 (m, 3H, ArH), 6.99–6.93 (m, 2H, ArH), 6.36–6.29 (m, 2H, ArH), 2.20 (s, 3H, CH_3); ^{13}C NMR (75 MHz, DMSO-d_6): δ 170.0, 159.1, 154.2, 150.2, 147.2, 139.0, 132.2, 131.5, 130.6, 128.4, 127.5, 125.9, 124.3, 123.3, 120.1, 118.8, 116.2, 114.6, 96.3, 23.9; anal. calcd for $C_{29}H_{19}N_3O_5S$: C, 66.77; H, 3.67; N, 8.05; S, 6.13; found: C, 66.69; H, 3.60; N, 8.01; S, 6.09.

(*E*)-*N*′-(3-(2,3-Dimethylphenyl)-4-(2-oxo-2*H*-chromen-3-yl)-thiazol-2(3*H*)-ylidene)-2-oxo-2*H*-chromene-3-carbohydrazide (5i). Yield: (65%); m.p.: 128–130 °C; R_f: 0.42; IR (ATR, cm^{-1}): 3312 (NH), 1717 (C=O), 1615 (C=N); ^{1}H NMR (300 MHz, DMSO-d_6): δ 11.143 (s, 1H, NH), 9.10 (s, 1H, H-4), 8.69 (s, 1H, H-4′), 7.96–7.84 (m, 4H, ArH), 7.69–7.49 (m, 4H, ArH), 7.43–7.40 (m, 1H, ArH), 6.99–6.96 (m, 2H, ArH), 6.65–6.59 (m, 1H, ArH), 2.23 (s, 3H, CH_3), 2.01 (s, 3H, CH_3); ^{13}C NMR (75 MHz, DMSO-d_6): δ 169.3, 159.7, 152.8, 150.3, 147.7, 141.1, 136.8, 131.3, 129.1, 128.4, 127.5, 126.6, 125.2, 124.7, 121.0, 120.0, 119.3, 118.3, 116.5, 114.7, 100.2, 23.5, 19.3; anal. calcd for $C_{30}H_{21}N_3O_5S$: C, 67.28; H, 3.94; N, 7.84; S, 5.98; found: C, 67.23; H, 3.90; N, 7.80; S, 5.93.

(*E*)-*N*′-(3-(2,4-Dimethylphenyl)-4-(2-oxo-2*H*-chromen-3-yl)thiazol-2(3*H*)-ylidene)-2-oxo-2*H*-chromene-3-carbohydrazide (5j). Yield: (71%); m.p.: 135–137 °C; R_f: 0.43; IR (ATR, cm^{-1}): 3296 (NH), 1717 (C=O), 1612 (C=N); ^{1}H NMR (300 MHz, DMSO-d_6): δ 11.02 (s, 1H, NH), 9.09 (s, 1H, H-4), 8.58 (s, 1H, H-4′), 7.93–7.87 (m, 2H, ArH), 7.83–7.74 (m, 2H, ArH), 7.61–7.59 (m, 1H, ArH), 7.37–7.19 (m, 4H, ArH), 6.96–6.91 (m, 1H, ArH), 6.73–6.65 (m, 2H, ArH), 2.34 (s, 3H, CH_3), 2.02 (s, 3H, CH_3); ^{13}C NMR (75 MHz, DMSO-d_6): δ 168.1, 158.5, 152.0, 151.6, 148.3, 143.8, 139.1, 137.4, 136.3, 133.2, 131.6, 130.4, 129.1, 127.3, 126.7, 125.5, 121.2, 119.3, 117.1, 114.7, 100.1, 26.3, 15.8; anal. calcd for $C_{30}H_{21}N_3O_5S$: C, 67.27; H, 3.95; N, 7.83; S, 5.97; found: C, 67.19; H, 3.84; N, 7.76; S, 5.83.

(*E*)-*N*′-(3-(2,6-Dimethylphenyl)-4-(2-oxo-2*H*-chromen-3-yl)-thiazol-2(3*H*)-ylidene)-2-oxo-2*H*-chromene-3-carbohydrazide (5k). Yield: (69%); m.p.: 152–154 °C; R_f: 0.46; IR (ATR, cm^{-1}): 3316 (NH), 1717 (C=O), 1607 (C=N); ^{1}H NMR (300 MHz, DMSO-d_6): δ 11.11 (s, 1H, NH), 9.39 (s, 1H, H-4), 9.00 (s, 1H, H-4′), 7.83–7.69 (m, 4H, ArH), 7.54–7.51 (m, 2H, ArH), 7.39–7.34 (m, 3H, ArH), 6.99–6.96 (m, 2H, ArH), 6.67–6.63 (m, 1H, ArH), 2.09 (s, 6H, 2 × CH_3); ^{13}C NMR (75 MHz, DMSO-d_6): δ 169.9, 157.2, 151.4, 150.3, 149.0, 147.4, 133.5, 130.6, 129.1, 128.6, 126.9, 125.4, 123.2, 121.7, 119.1, 118.8, 116.3, 114.5, 99.0, 17.6; anal. calcd for $C_{30}H_{21}N_3O_5S$: C, 67.27; H, 3.95; N, 7.83; S, 5.97; found: C, 67.20; H, 3.89; N, 7.79; S, 5.86.

(*E*)-*N*′-(3-(3,4-Dimethylphenyl)-4-(2-oxo-2*H*-chromen-3-yl)thiazol-2(3*H*)-ylidene)-2-oxo-2*H*-chromene-3-carbohydrazide (5l). Yield: (67%); m.p.: 109–111 °C; R_f: 0.42; IR (ATR, cm^{-1}): 3329 (NH), 1723 (C=O), 1629 (C=N); ^{1}H NMR (300 MHz, DMSO-d_6): δ 11.14 (s, 1H, NH), 9.01 (s, 1H, H-4), 8.67 (s, 1H, H-4′), 7.97–7.92 (m, 1H, ArH), 7.81–7.69 (m, 2H, ArH), 7.63–7.57 (m, 1H, ArH), 7.48–7.20 (m, 4H, ArH), 7.12–7.02 (m, 1H, ArH), 6.99–6.93 (m, 1H, ArH), 6.89–6.80 (m, 2H, ArH), 2.22 (s, 3H, CH_3), 2.10 (s, 3H, CH_3); ^{13}C NMR (75 MHz, DMSO-d_6): δ 168.1, 158.2, 151.1, 149.0, 147.7, 140.1, 137.8, 131.5, 130.2, 129.6, 127.3, 126.8, 125.2, 123.7, 121.0, 119.7, 118.4, 116.3, 115.1, 114.8, 99.0, 20.8, 18.1; anal. calcd for $C_{30}H_{21}N_3O_5S$: C, 67.26; H, 3.93; N, 7.81; S, 5.96; found: C, 67.20; H, 3.87; N, 7.75; S, 5.89.

(*E*)-*N*′-(3-(3,5-Dimethylphenyl)-4-(2-oxo-2*H*-chromen-3-yl)thiazol-2(3*H*)-ylidene)-2-oxo-2*H*-chromene-3-carbohydrazide (5m).

Yield: (66%); m.p.: 125–128 °C; R_f: 0.40; IR (ATR, cm^{-1}): 3293 (NH), 1715 (C=O), 1618 (C=N); ^1H NMR (300 MHz, DMSO-d_6): δ 11.13 (s, 1H, NH), 9.10 (s, 1H, H-4), 8.89 (s, 1H, H-4′), 7.83–7.71 (m, 2H, ArH), 7.68–7.63 (m, 1H, ArH), 7.42–7.31 (m, 4H, ArH), 7.07–7.00 (m, 2H, ArH), 6.95–6.89 (m, 1H, ArH), 6.65–6.53 (m, 2H, ArH), 2.31 (s, 6H, 2 × CH_3); ^{13}C NMR (75 MHz, DMSO-d_6): δ 169.2, 158.1, 154.0, 151.6, 147.2, 141.3, 137.7, 131.5, 129.0, 128.1, 126.7, 125.2, 123.1, 121.8, 120.5, 118.7, 116.9, 114.3, 96.9, 24.3; anal. calcd for $C_{30}H_{21}N_3O_5S$: C, 67.26; H, 3.93; N, 7.81; S, 5.96; found: C, 67.23; H, 3.85; N, 7.77; S, 5.83.

Pharmacological protocols

Alkaline phosphatase inhibition. Newly synthesized bis-coumarin–thiazole compounds were tested against calf intestinal alkaline phosphatase (CIAP). The compounds were initially tested against these enzymes at 10 μM concentration to further make a dose-response curve of potential inhibitors of synthesized compounds by using previously described method by J. Iqbal.[45] The solution was made in assay buffer (pH 9.5) comprises of tris-hydrochloride (50 mM), $MgCl_2$ (5 mM), $ZnCl_2$ (0.1 mM) and glycerol 50% in the solution. The solution of enzyme substrate *p*-nitrophenyl phosphate (*p*-NPP) and test compounds was also prepared in the same buffer without glycerol. The assay was started in 96 wells plate by adding 70 μL of assay buffer, 10 μL of test compound (from 100 μM compound stock solution), 10 μL of optimized enzyme (0.5 U mL^{-1}) and then incubated at 37 °C for 10 minutes. To initialize the reaction a 10 μL of substrate (5 mM *p*-NPP) was added into each well and again incubated for additional 30 minutes. The change in absorbance of released *p*-nitrophenolate was monitored at 405 nm, using a 96-well microplate reader (Bio-Tek ELx 800 TM, Instruments, Inc. USA). The percent inhibition of each compound was calculated by comparing the results with the control wells having no inhibitor at all. The compounds which showed ≥50% inhibition were selected for further determination of dose-response curves against all compounds. For this purpose 7–9 serial dilutions of each compound spanning three orders of magnitude were prepared in enzyme assay buffer and their dose response curves were obtained by adopting the same methods used for initial screening. All experiments were repeated three times in triplicate. Results reported are mean of three independent experiments (±SEM) and expressed as percent inhibitions calculated by the formula;

$$\text{Inhibition (\%)} = [100 - (\text{abs of test compound/abs of control}) \times 100]$$

IC_{50} values of selected compounds exhibiting >50% activity at 0.5 mM were calculated after dilutions using computer program GraphPad, San Diego, California, USA.

Leishmanicidal assay

Parasite and culture. *Leishmania major* promastigotes were cultured at 25 ± 1 °C to logarithmic phase in D-MEM/F-12 medium (Gibco BRL) without phenol red, supplemented by 10% heat inactivated fetal bovine serum (FBS), 100 IU mL^{-1} penicillin and 100 μg mL^{-1} streptomycin, then washed 3 times with PBS by centrifugation at 1500 rpm for 10 min at room temperature and resuspended at a concentration of 2.5 × 10^6 parasites per mL in medium.

Antileishmanial activity assay (MTT assay). The antileishmanial activity of the newly synthesized compounds was evaluated *in vitro* against the promastigote forms of *Leishmania major* using a MTT (3-(4,5-dimethylthiazol-2yl)-2,5-diphenyltetrazoliumbromide)-based microassay as a marker of cell viability. The MTT assay used was based on that originally described by Mosmann[46] modified by Niks and Otto.[47] A stock solution of MTT (Sigma Chemical Co., St. Louis, Mo.) was prepared by dissolving in PBS at 5 mg mL^{-1} and storing in the dark at 4 °C for up to 2 weeks before use. For the antileishmanial activity assays, 100 μL per well of the culture which contained 2.5 × 10^6 cells per mL promastigotes was seeded in 96-well flat-bottom plates. Then, 10 μL per well from various concentrations of synthesized compounds were added to triplicate wells and plates were incubated for 72 h at 25 ± 1 °C. The first well of 96 wells was as a blank well which only contained of 100 μL culture medium without any compound, drug or parasite. Amphotericin B was used as standard drug. At the end of incubation, 10 μL of MTT was added to each well and plates were incubated for 3 h at 25 ± 1 °C. Enzyme reaction was then stopped by the addition of 100 μL of 50% isopropanol and 10% sodium dodecyl sulfate. The plates were incubated for an additional 30 min under agitation at room temperature. Relative optical density (OD) was then measured at a wavelength of 570 nm using a 96-well microplate reader (Bio-Tek ELx 800 TM, Instruments, Inc. USA). The background absorbance of plates was measured at 690 nm and subtract from 570 nm measurement. The absorbance of the formazan produced by the action of mitochondrial dehydrogenases of metabolically active cells is shown to correlate with the number of viable cells. All experiments were repeated at least three times. Results reported are mean of three independent experiments (±SEM) and expressed as percent inhibitions calculated by the formula:

$$\text{Inhibition (\%)} = [100 - (\text{abs of test compound/abs of control}) \times 100]$$

Cytotoxicity assay

Cell lines and cultures. Lung carcinoma (H-157), (ATCC CRL-5802) and kidney fibroblast (BHK-21), (ATCC CCL-10) cell lines were kept in RPMI-1640 [having heat-inactivated fetal bovine serum (10%) glutamine (2 mM), pyruvate (1 mM), 100 U mL^{-1} penicillin and 100 μg mL^{-1} streptomycin] in T-75 cm^2 sterile tissue culture flasks in a 5% CO_2 incubator at 37 °C.[53] 96-well plates were used for growing H-157 and BHK-21 cells by inoculating 10^4 cells per 100 μL per well and plates were incubated in CO_2 incubator. Within 24 h, a uniform monolayer was formed which was used for experiments.

Cytotoxicity analysis by sulforhodamine B (SRB) assay. To perform cytotoxicity assay with H-157 and BHK-21 cells, a previously described method by Skehan *et al.*,[48] was adopted with some modifications. Briefly, cells were cultured in

different 96 well plates for 24 h. The compounds in different concentrations (100, 10, 1 and 0.1 μM) were inoculated in test wells while control and blank wells were also prepared containing standard drug (vincristine) and culture media with cells, respectively. The plates were then incubated for 48 h. After that cells were fixed with 50 μL of 50% ice cold trichloroacetic acid solution (TCA) at 4 °C for 1 h. The plates were washed 5 times with phosphate-buffered saline (PBS) and air dried. Fixed cells were further treated with 0.4% w/v sulforhodamine B dye prepared in 1% acetic acid solution and left at room temperature for 30 min. After that the plates were rinsed with 1% acetic acid solution and allowed to dry. In order to solubilize the dye, the dried plates were treated with 10 mM Tris base solution for 10 min at room temperature. Absorbance was measured at 490 nm subtracting the background measurement at 630 nm.[54] All experiments were repeated at least three times. Results reported are mean of three independent experiments (±SEM) and expressed as percent inhibitions calculated by the formula:

$$\text{Inhibition (\%)} = [100 - (\text{abs of test compound/abs of control}) \times 100]$$

Molecular docking

Preparation of receptor. The crystal structure of alkaline phosphate (PDB code: 4KJG)[51] was retrieved from protein data bank with its cognate ligand and active site was found around the cognate ligand by using Lig X module of MOE.

Preparation of ligands. The ligand files for molecular docking studies were prepared in molecular operating environment (MOE) by chemical computing group (CCG).[55] Drawn geometries were followed by energy optimization at standard MMFF94 force field level, with a 0.0001 kcal mol^{-1} energy gradient convergence criterion.[49] These ligands were saved in molecular data base file for docking studies.

Druglikeness and molecular docking studies. Physical descriptors were calculated by making use of the "Descriptor module" of MOE program to gauge the druglikeness of all the compounds. The optimized ligands were docked with the IALP (PDB code: 4KJG) protein using the MOE-Dock program. A total of 20 independent docking runs were performed using MOE docking simulation program. The best scored pose (minimum energy) for each compound was retained for further studies of interaction evaluation. The 2D ligand–protein interactions were visualized using the MOE ligand interactions program. Detailed docking results are recorded in Table S2 given in ESI.†

Acknowledgements

A. I is grateful to the Higher Education Commission of Pakistan for the financial support under Indigenous 5000 PhD Fellowship Program. We are thankful to Dr Charles Dennis Hall and Prof. Alan R. Katritzky (late) (University of Florida) for the MOE software license. The Department of Energy, United State of America, is gratefully acknowledged for support through Grant No. DE-SC0001717.

References

1 M. H. le Du and J. L. Millan, *J. Biol. Chem.*, 2002, **277**, 49808–49814.
2 L. Zhang, M. Balcerzak, J. Radisson, C. Thouverey, S. Pikula, G. Azzar and R. Buchet, *J. Biol. Chem.*, 2005, **280**, 37289–37296.
3 S. P. Coburn, J. D. Mahuren, M. Jain, Y. Zubovic and J. Wortsman, *J. Clin. Endocrinol. Metab.*, 1998, **83**, 3951–3957.
4 D. Sarrouilhe, P. Lalegerie and M. Baudry, *Biochim. Biophys. Acta*, 1992, **1118**, 116–122.
5 M. Muda, N. N. Rao and A. Torriani, *J. Bacteriol.*, 1992, **174**, 8057–8064.
6 M. Li, W. Ding, B. Baruah, D. C. Crans and R. Wang, *J. Inorg. Biochem.*, 2008, **102**, 1846–1853.
7 G. R. Mundy, *Nat. Rev. Cancer*, 2002, **2**, 584–593.
8 G. D. Roodman, *N. Engl. J. Med.*, 2004, **350**, 1655–1664.
9 C. J. Logothetis and S.-H. Lin, *Nat. Rev. Cancer*, 2005, **5**, 21–28.
10 K. Jung, M. Lein, C. Stephan, K. von Hösslin, A. Semjonow, P. Sinha, S. A. Loening and D. Schnorr, *Int. J. Cancer*, 2004, **111**, 783–791.
11 D. Sloane, *Methods Mol. Biol.*, 2009, **471**, 65–83.
12 M. Mareel and A. Leroy, *Physiol. Rev.*, 2003, **83**, 337–376.
13 J. Weschel, K. Haglund and E. M. Haugsten, *Biochem. J.*, 2011, **437**, 199–213.
14 J. Cummings, T. H. Ward, M. Ranson and C. Dive, *Biochim. Biophys. Acta*, 2004, **1705**, 53–66.
15 WHO, *Research Priorities for Chagas Disease, Human African Trypanosomiasis and Leishmaniasis*, WHO Technical Report Series No. 975, 2012, p. 116.
16 C. R. Davies, R. P. Kaye, S. L. Croft and S. Sundar, *BMJ [Br. Med. J.]*, 2003, **15**, 377–382.
17 P. Trouiller, E. Torreele, P. Olliaro, N. White, S. Foster, D. Wirth and B. Pécoul, *Trop. Med. Int. Health*, 2001, **6**, 945–951.
18 J. Alvar, I. D. Vélez, C. Bern, M. Herrero, P. Desjeux, J. Cano, J. Jannin and M. den Boer, *PLoS One*, 2012, **7**, e35671.
19 *Working to Overcome the Global Impact of Neglected Tropical Diseases, First WHO Report on Neglected Tropical Diseases*, ed. D. W. T. Compton and P. Peters, World Health Organization, Geneva, 2010.
20 (*a*) V. Polshettiwar and R. S. Varma, *Curr. Opin. Drug Discovery Dev.*, 2007, **10**, 723–737; (*b*) I. Khan, A. Ibrar, N. Abbas and A. Saeed, *Eur. J. Med. Chem.*, 2014, **76**, 193–244.
21 (*a*) A. Padwa and S. K. Bur, *Tetrahedron*, 2007, **63**, 5341–5378; (*b*) I. Khan, A. Ibrar, W. Ahmed and A. Saeed, *Eur. J. Med. Chem.*, 2015, **90**, 124–169.
22 D. M. D'Souza and T. J. Muller, *Chem. Soc. Rev.*, 2007, **36**, 1095–1108.
23 G. Eren, S. Unlu, M. T. Nunez, L. Labeaga, F. Ledo, A. Entrena, E. B. Lu, G. Costantino and M. F. Sahin, *Bioorg. Med. Chem.*, 2010, **18**, 6367–6376.
24 R. J. Gillespie, A. I. Cliffe, C. E. Dawson, C. T. Dourish, S. Gaur, P. R. Giles, A. M. Jordan, A. R. Knight, A. Lawrence, J. Lerpiniere, A. Misra, R. M. Pratt,

R. S. Todd, R. Upton, S. M. Weiss and D. S. Williamson, *Bioorg. Med. Chem. Lett.*, 2008, **18**, 2920–2923.
25 V. Jaishree, N. Ramdas, J. Sachin and B. Ramesh, *J. Saudi Chem. Soc.*, 2012, **16**, 371–376.
26 A. T. Ricardo, A. Luz and D. P. Carlos, *Bioorg. Med. Chem.*, 2003, **11**, 2175–2182.
27 A. Zablotskaya, I. Segal, A. Geronikaki, T. Eremkina, S. Belyakov, M. Petrova, I. Shestakova, L. Zvejniece and V. Nikolajeva, *Eur. J. Med. Chem.*, 2013, **70**, 846–856.
28 M. H. M. Helal, M. A. Salem, M. S. A. El-Gaby and M. Aljahdali, *Eur. J. Med. Chem.*, 2013, **65**, 517–526.
29 R. Romagnoli, P. G. Baraldi, M. K. Salvador, M. E. Camacho, D. Preti, M. A. Tabrizi, M. Bassetto, A. Brancale, E. Hamel, R. Bortolozzi, G. Basso and G. Viola, *Bioorg. Med. Chem.*, 2012, **20**, 7083–7094.
30 K. N. Venugopala, M. Krishnappa, S. K. Nayak, B. K. Subrahmanya, J. P. Vaderapura, R. K. Chalannavar, R. M. Gleiser and B. Odhav, *Eur. J. Med. Chem.*, 2013, **65**, 295–303.
31 (*a*) A. Saeed and A. Ibrar, *Phosphorus, Sulfur Silicon Relat. Elem.*, 2011, **186**, 1801–1810; (*b*) A. Raza, A. Saeed, A. Ibrar, M. Muddassar, A. A. Khan and J. Iqbal, *ISRN Pharmacol.*, 2012, **2012**, 1–11; (*c*) A. Saeed, P. A. Channar, Q. Iqbal and J. Mahar, *Chin. Chem. Lett.*, 2015, DOI: 10.1016/j.cclet.2015.09.011.
32 O. Dömötör, T. Tuccinardi, D. Karcz, M. Walsh, B. S. Creaven and É. A. Enyedy, *Bioorg. Chem.*, 2014, **52**, 16–23.
33 Y. Zhao, Q. Zheng, K. Dakin, K. Xu, M. L. Martinez and W.-H. Li, *J. Am. Chem. Soc.*, 2004, **126**, 4653–4663.
34 J. R. Hwu, S.-Y. Lin, S.-C. Tsay, E. de Clercq, P. Leyssen and J. Neyts, *J. Med. Chem.*, 2011, **54**, 2114–2126.
35 S.-C. Tsay, J. R. Hwua, R. Singha, W.-C. Huang, Y. H. Chang, M. H. Hsu, F.-K. Shieh, C.-C. Lin, K. C. Hwang, J. C. Horng, E. de Clercq, I. Vliegen and J. Neyts, *Eur. J. Med. Chem.*, 2013, **63**, 290–298.
36 K. Nepali, S. Sharma, M. Sharma, P. M. S. Bedi and K. L. Dhar, *Eur. J. Med. Chem.*, 2014, **77**, 422–487.
37 F. W. Muregi and A. Ishih, *Drug Dev. Res.*, 2010, **71**, 20–32.
38 C. Hubschwerlen, J. L. Specklin, C. Sigwalt, S. Schroeder and H. H. Locher, *Bioorg. Med. Chem.*, 2003, **11**, 2313–2319.
39 R. Pingaew, S. Prachayasittikul, S. Ruchirawat and V. Prachayasittikul, *Med. Chem. Res.*, 2014, **23**, 1768–1780.
40 (*a*) K. V. Sashidhara, R. K. Modukuri, S. Singh, K. B. Rao, G. A. Teja, S. Gupta and S. Shukla, *Bioorg. Med. Chem. Lett.*, 2015, **25**, 337–341; (*b*) K. V. Sashidhara, S. R. Avula, K. Sharma, G. R. Palnati and S. R. Bathula, *Eur. J. Med. Chem.*, 2013, **60**, 120–127; (*c*) K. V. Sashidhara, R. K. Modukuri, D. Choudhary, K. B. Rao, M. Kumar, V. Khedgikar and R. Trivedi, *Eur. J. Med. Chem.*, 2013, **70**, 802–810; (*d*) F. Belluti, G. Fontana, L. D. Bo, N. Carenini, C. Giommarelli and F. Zunino, *Bioorg. Med. Chem.*, 2010, **18**, 3543–3550; (*e*) Q. Sun, D.-Y. Peng, S.-G. Yang, X.-L. Zhu, W.-C. Yang and G.-F. Yang, *Bioorg. Med. Chem.*, 2014, **22**, 4784–4791; (*f*) K. Paul, S. Bindal and V. Luxami, *Bioorg. Med. Chem. Lett.*, 2013, **23**, 3667–3672; (*g*) R. Aggarwal, S. Kumar, P. Kaushik, D. Kaushik and G. K. Gupta, *Eur. J. Med. Chem.*, 2013, **62**, 508–514.
41 (*a*) I. Khan, S. Zaib, A. Ibrar, N. H. Rama, J. Simpson and J. Iqbal, *Eur. J. Med. Chem.*, 2014, **78**, 167–177; (*b*) I. Khan, S. J. A. Shah, S. A. Ejaz, A. Ibrar, S. Hameed, J. Lecka, J. L. Millan, J. Sévigny and J. Iqbal, *RSC Adv.*, 2015, **5**, 64404–64413.
42 (*a*) I. Khan, A. Ibrar, S. Zaib, S. Ahmad, N. Furtmann, S. Hameed, J. Simpson, J. Bajorath and J. Iqbal, *Bioorg. Med. Chem.*, 2014, **22**, 6163–6173; (*b*) I. Khan, S. M. Bakht, A. Ibrar, S. Abbas, S. Hameed, J. M. White, U. A. Rana, S. Zaib, M. Shahid and J. Iqbal, *RSC Adv.*, 2015, **5**, 21249–21267; (*c*) A. Saeed, P. A. Channar, Q. Iqbal and J. Mahar, *Chin. Chem. Lett.*, DOI: 10.1016/j.cclet.2015.09.011.
43 T. Somerai, L. Szilagyi and S. Horvath, *Arch. Pharm.*, 1986, **139**, 238–241.
44 K. M. Dawood, H. Abdel-Gawad, H. A. Mohamed and F. A. Badria, *Med. Chem. Res.*, 2011, **20**, 912–919.
45 J. Iqbal, *Anal. Biochem.*, 2011, **414**, 226–231.
46 T. Mosmann, *J. Immunol. Methods*, 1983, **65**, 55–63.
47 M. Niks and M. Otto, *J. Immunol. Methods*, 1990, **130**, 149–151.
48 P. Skehan, R. Storeng, D. Scudiero, A. Monks, J. McMahon, D. Vistica, J. T. Warren, H. Bokesch, S. Kenney and M. R. Boyd, *J. Natl. Cancer Inst.*, 1990, **82**, 1107–1112.
49 D. F. Veber, S. R. Johnson, H.-Y. Cheng, B. R. Smith, K. W. Ward and K. D. Kopple, *J. Med. Chem.*, 2002, **45**, 2615–2623.
50 C. A. Lipinski, F. Lombardo, B. W. Dominy and P. Feeney, *Adv. Drug Delivery Rev.*, 1997, **23**, 3–25.
51 K. Ghosh, T. D. Mazumde, R. Anumula, B. Lakshmaiah, P. P. Kumar, S. Singaram, T. Matan, S. Kallipatti, S. Selyam, P. Krishnamurthy and M. Ramarao, *J. Struct. Biol.*, 2013, **184**, 182–192.
52 N. Ingale, V. Maddi, M. Palkar, P. Ronad, S. Mamledesai, A. H. M. Vishwanathswamy and D. Satyanarayana, *Med. Chem. Res.*, 2012, **21**, 16–26.
53 K. Araki-Sasaki, S. Aizawa, M. Hiramoto, M. Nakamura, O. Iwase, K. Nakata, Y. Sasaki, T. Mano, H. Handa and Y. Tano, *J. Cell. Physiol.*, 2000, **182**, 189–195.
54 G. S. Longo-Sorbello, G. m. Say, D. Banerjee and J. R. Bertino, Cytotoxicity and cell growth assays, *Cell Biology, Four-Volume Set: A Laboratory Handbook*, 2005, vol. 1, pp. 315–324.
55 *Molecular Operating Environment (MOE), 2013.08*, Chemical Computing Group Inc., 1010, Sherbooke St. West, Suite #910, Montreal, QC, Canada, H3A 2R7, 2015.